[6] Bogoliubof, N. N. and Mitropolsky, Y. A., *Asymptotic Methods in the Theory of Nonlinear Oscillations*, Gordon and Breach Scientific Publications, New York, 1961.

[7] Volosov, V. M., "The Method of Averaging," *Soviet Mathematics Doklady*, Vol. 2, No. 2, March 1961, pp. 221–224.

[8] Volosov, V. M., "Higher Approximations in Averaging," *Soviet Mathematics Doklady*, Vol. 2, No. 2, March 1961, pp. 382–385.

[9] Schwausch, O. A., "Subroutine STEPER, A FORTRAN Subroutine for the Numerical Integration of First-Order Ordinary Differential Equations Using Either a Fixed or Variable Integration Step Size," Contract NAS 9-5384, April 1969, Lockheed Electronics Co., Houston, Texas.

[10] Battin, R. H., *Astronautical Guidance*, McGraw-Hill, New York, 1964, pp. 198–199.

Effect of Base Mounted Cylinders on a Supersonic Near Wake

RICHARD A. MERZ,* ROBERT H. PAGE,† AND CHRISTIAN E. G. PRZIREMBEL‡
Rutgers University, New Brunswick, N.J.

Nomenclature

D = base diameter
d = cylinder diameter
F_b = force on annular base
F_s = force on cylinder
L = cylinder length
M = freestream Mach number
n = boundary-layer velocity power law coefficient
p_b = base pressure
p_e = equivalent base pressure [Eq. (1)].
p_o = freestream stagnation pressure
p_s = base pressure on cylinder
R = Reynolds number
T_0 = freestream stagnation temperature
δ = boundary-layer thickness
δ^* = displacement thickness
θ = momentum thickness

Introduction

NUMEROUS experimental investigations of axisymmetric base flow regions have shown that the low pressure recirculation region associated with blunt based supersonic vehicles contributes significantly to the total drag of the body. Since most wind-tunnel measurements of base pressure and/or drag have been made with sting mounted models, the effect of base mounted cylinders or protuberances on the recirculation flowfield has been discussed and debated by many investigators. Furthermore, the influence of instrumentation booms mounted in the wake of free-flight vehicles has been of recent interest. Sieling and Page[1,2] have reviewed much of the available experimental literature. Their results have indicated a need for a systematic study of the effect of various protuberances on the near wake flow properties.

Presented as Paper 72-1013 at the AIAA 7th Aerodynamic Testing Conference, Palo Alto, Calif., September 13–15, 1972; submitted September 28, 1972; revision received February 9, 1973. Research jointly sponsored by the Air Force Office of Scientific Research, Office of Aerospace Research, United States Air Force, under Contract F44620-68-C-0018; the Undergraduate Research Participation Program of the National Science Foundation under Grant GY-6054, and Rutgers University.

Index categories: Jets, Wakes, and Viscid-Inviscid Flow Interaction; Rocket Vehicle Aerodynamics; Re-entry Vehicle Testing.

*Research Intern. Student Member AIAA.

†Professor and Chairman, Department of Mechanical, Industrial and Aerospace Engineering. Associate Fellow AIAA.

‡Associate Professor. Member AIAA.

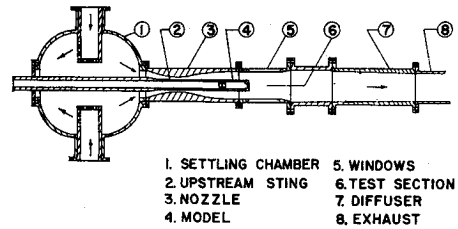

Fig. 1. Schematic of RANT.

Apparatus

A series of tests was conducted in the Rutgers Axisymmetric Near Wake Tunnel (RANT)[3] which was specifically designed for studies of supersonic turbulent axisymmetric near wakes in the absence of supports or freestream disturbances. As shown in Fig. 1, the unique feature of RANT is an upstream sting which was designed as an integral part of the nozzle to produce a uniform flow over a model of 76.2mm diam. The freestream test conditions were $M = 3.88$, $R = 5.12 \times 10^7$/m, $p_0 = 105.2$ nt/cm^2, and $T_0 = 293°\,K \pm 10°\,K$. The turbulent boundary layer on the base model had the following measured properties: $n = 7.3$, $\delta = 8.75$mm, $\delta^* = 3.56$mm, $\theta = 0.435$mm. Short cylinders were attached to the base of the tunnel's upstream sting. Figure 2 shows a schematic of the model configuration.

Ten different diameter cylinders were tested. The ratio of cylinder diameter to model diameter (d/D) varied between 0.083 and 0.666. The length of each cylinder was varied from a full length of approximately two base diameters to zero length in small increments to insure that data were obtained throughout the significant points of the near wake region.

For each test, the cylinder was screwed into a blunt base of 76.2 mm diam. making sure no leaks were present. Four pressure taps, equally spaced around the circumference of the model and located 4mm upstream from the base, permitted the freestream static pressure to be measured. Equal pressure readings from these taps insured that the model was aligned properly and the flow was indeed axisymmetric. Six pressure taps on the base were used to measure the pressure acting on the base. Two taps were each located at radii 20.6, 27.0 and 34.9mm. A final pressure tap was located at the center of the cylinder base. All the pressure taps had a diameter of 0.71mm.

All the pressure measurements were made with a Statham 0–5.2 nt/cm^2 transducer and a Scanivalve. The signal was recorded as a deflection on an x-y plotter. The transducer, Scanivalve and recorder were calibrated as a instrumentation system with a Texas Instrument precision pressure gage. All

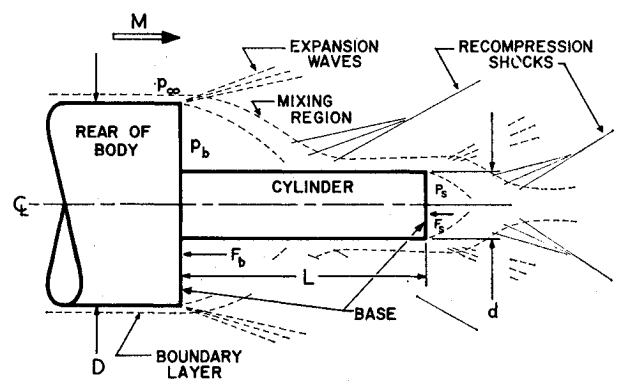

Fig. 2. Model configuration and flow pattern.

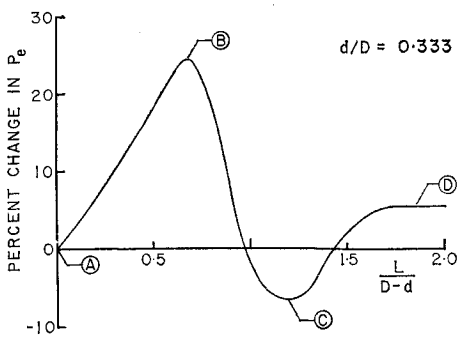

Fig. 3. Effect of cylinder length on equivalent base pressure.

system pressure measurements were accurate to ± 0.007 nt/cm^2.

Results

In order to determine the effect of the base mounted cylinder on the drag, an equivalent base pressure was defined as follows

$$p_e = p_b[1 - (d^2/D^2)] + p_s d^2/D^2 \quad (1)$$

Thus when the equivalent pressure is multiplied by the model base area, it produces the same force on the base as that obtained with the cylinder present (Fig. 2). This quantity was compared to the pressure on a plain blunt base. The percentage change in equivalent pressure was plotted against the dimensionless length of the cylinder. The step height, i.e., $(D - d)$, was used to normalize the cylinder length.

A typical plot of percentage change in equivalent pressure vs the dimensionless length of the cylinder is shown in Fig. 3. This particular case, for which $d/D = 0.333$, displays the trends that were found for all cases in which $d/D \geq 0.250$. For all these cases, a maximum increase in equivalent pressure is found for dimensionless lengths between 0.3 and 0.7 while a local minimum is found for lengths between 0.9 and 1.2. As the length scale exceeds 1.5, a constant value of equivalent pressure is achieved for each cylinder diameter.

Color schlieren photographs were taken for each configuration tested by replacing the conventional schlieren knife edge with a tricolor filter. Significant flowfield changes observed by this technique are marked A, B, C and D, respectively, in Fig. 3. For instance, at point C, the primary free shear layer has attached to the cylinder. As the cylinder length is increased, the secondary expansion region and recompression shocks become quite visible. The photographs also showed that beyond point D in Fig. 3 there is no further change in the flow structure.

Composite plots of the results from 180 tested conditions are presented in Figs. 4 and 5. A 30% increase in equivalent

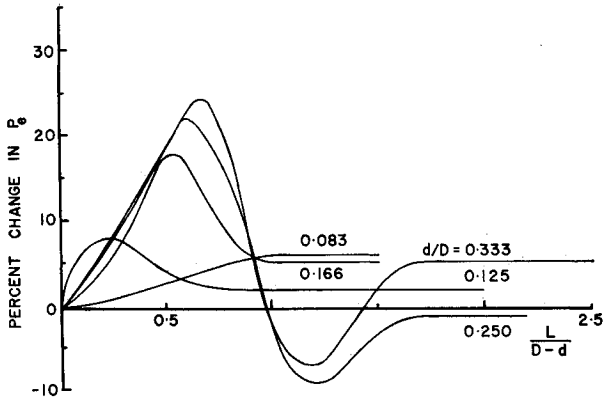

Fig. 4 Equivalent base pressure vs cylinder length.

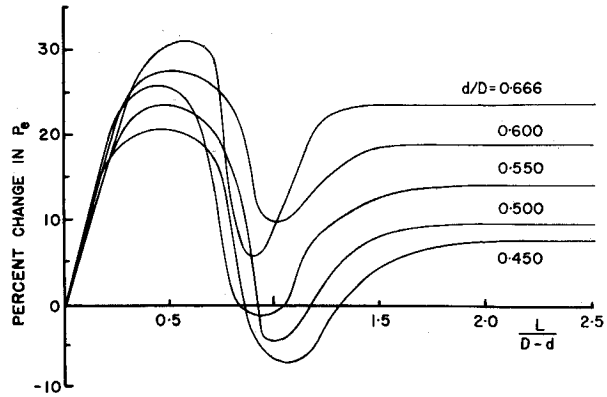

Fig. 5. Equivalent base pressure vs cylinder length.

base pressure was the maximum change recorded. It occurred for the geometrical configuration of $d/D = 0.666$ and $L/(D - d) = 0.600$. In some cases, the cylinder caused a negative change in the equivalent pressure, i.e., an increase in base drag. For example, with $d/D = 0.250$ and $L/(D - d) = 1.200$, the equivalent pressure decreased by approximately 10%.

The cases for d/D equal to 0.083 and 0.125 show a length effect which is not as pronounced as for the larger diameter cylinders. This agrees with previous data which show that small diameter stings do not affect the base drag to any great extent.[4]

Detailed analysis of the two contributing base forces showed, for the case of $d/D = 0.333$, that the force on the cylinder (F_s) increased only slowly as the cylinder was lengthened, and was significantly less than the base force on the annulus. However, the base force on the annulus (F_b) changes with cylinder length, having distinct maximum and minimum points at $L/(D - d) = 0.650$ and 1.15, respectively. Hence, it is the change in annulus base pressure with cylinder length which dominates the equivalent base pressure, as shown in Fig. 4. On the other hand, for $d/D = 0.666$, it is the base force on the cylinder which makes the major contribution to the total force (i.e., equivalent base pressure). This is primarily due to the increased area over which the sting pressure acts. However, as in the previous case, it is the change in annulus base pressure which determines the maximum and minimum points in the total force.

Conclusions

A detailed experimental investigation of the influence of base mounted cylinders on the near wake of an axisymmetric blunt based body has been completed. The data show that the near wake is significantly influenced by short base mounted cylinders. Indeed, a large increase in base force and consequently a decrease in base drag can be obtained by the careful selection of the geometry of a base cylinder. A maximum increase in equivalent pressure of 30% was observed for $d/D = 0.666$ and $L/(D - d) = 0.600$. The effects on the flow pattern are in general agreement with the theoretical understanding of supersonic near wakes.[5]

References

[1]Sieling, W. R., "The Effect of Sting Diameter and Length on Base Pressure at $M = 3.88$," *Aeronautical Quarterly*, Vol. XIX, Nov. 1968, pp. 368–374.

[2]Sieling, W. R. and Page, R. H., "A Re-Examination of Sting Interference Effects," AIAA Paper 70-585, Tullahoma, Tenn., 1970.

[3]Page, R. H., Dixon, R. J., and Przirembel, C.E.G., "Apparatus for Studies of Supersonic Axisymmetric Base Flow," *Proceedings of XVIIth International Astronautical Congress*, International Astronautical Federation, Madrid, Spain, Oct. 1966, pp. 347–353.

[4]Chapman, D. R., "An Analysis of Base Pressure at Supersonic

Velocities and Comparison with Experiment," Rept. 1051, 1951, NACA.

[5]Przirembel, C.E.G., and Page, R. H., "Analysis of Axisymmetric Supersonic Turbulent Base Flow," *Proceedings of the* 1968 *Heat Transfer and Fluid Mechanics Institute*, Stanford University Press, Stanford, Calif., 1968, pp. 258–272.

A Low-Power MPD Thruster of Duoplasmatron Type

ITSURO KIMURA* AND RYUHEI KUMAZAWA†
University of Tokyo, Tokyo, Japan

IN the past decade many studies have been made of low-thrust thrusters for such missions as satellite station-keeping or attitude control. Recently some promising experimental results were reported for low-thrust plasma thrusters (steady or pulsed), which are physically and electrically simpler than electrostatic thrusters (ion or colloid) and reliable in operation.[1,2]

The Duoplasmatron, an arc-type plasma source due to M. von Ardenne,[3] has been used as an ion source for electrostatic thrusters.[4,5] This plasma source, with a baffle (Zwischenelektrod) and a magnetic coil, can be operated at high-ionization efficiency (low neutral emission) with a variety of propellants, by means of the effect of mechanical or thermal constriction and magnetic constraint. This Note is concerned with the development of a simple low-thrust plasma thruster, composed of a Duoplasmatron-type plasma source and a magnetic nozzle. In the present device, the magnetic nozzle is produced by the same magnetic coil used in the plasma source (Fig. 1). The results of the experiment with hydrogen propellant show moderate thrust efficiencies in the range of relatively high specific impulse. Although the background pressure is not sufficiently low to obtain accurate data of the performance of the thruster, these experimental results demonstrate its capability as a low-thrust plasma thruster.

Apparatus and Experimental Procedure

The performance of the thruster depends sensitively upon the shape of the baffle (mild steel) and the anode (copper).

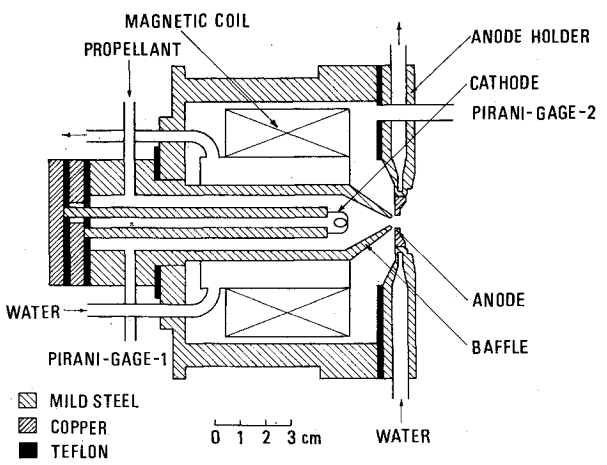

Fig. 1 Schematic of MPD thruster of Duoplasmatron-type.

Received October 20, 1972; revision received March 2, 1973.
Index category: Electric and Advanced Space Propulsion.
* Professor, Department of Aeronautics, Faculty of Engineering.
† Graduate Student, Graduate School of Aeronautics.

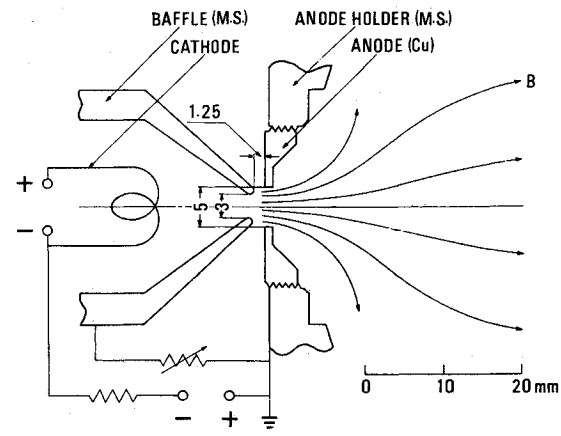

Fig. 2 Detail of electrode arrangement and magnetic field map.

The arrangement shown in Fig. 2 was finally adopted in the present experiment. This arrangement of the baffle and the anode holder (mild steel) permits shaping of the magnetic field (magnetic nozzle) such that it diverges in the exhaust region, when electric current flows through the magnetic coil. The magnetic field map in the figure was obtained by using iron filings. The average density of magnetic flux is of the order of 3000 gauss (coil current: 2.5 amp) at the throat of the magnetic nozzle.

In the present device with the thermionic cathode, the arc discharge can be initiated without any auxiliary equipment.[5] In the steady operation of the thruster, the baffle is maintained slightly positive of floating potential. The arc discharge produced is constricted by the baffle canal with throat of 3 mm diam (mechanical or thermal constriction), and the axial magnetic field between the baffle-tip and the anode further constrains the discharge (magnetic constraint). The combined effect causes formation of a cloud of hot dense plasma, which is expelled through the anode orifice of 5 mm diam and expands in the magnetic nozzle. The thruster has been operated mainly with hydrogen propellant, although some preliminary operations with argon propellant were also made. The gas pressure measured by Pirani gage 1 and 2 (Fig. 1) are of the order of 0.5 and 0.1 torr, respectively, for ordinary operating conditions.

The experiment was conducted in a 25-cm-diam by 40-cm-long bell jar, and the background pressure was maintained at about 2.5×10^{-3} torr (H_2 flow rate: 0.028 mg/sec) or 3×10^{-2} torr (H_2 flow rate: 0.033 mg/sec). It is reported that the background gas interferes with the normal thrust-producing mechanism, reducing the exhaust velocity, and also that it is entrained and accelerated by the thruster.[6] The experimental results shown in Ref. 6 suggest that the background pressure in the present experiment is not sufficiently low to obtain accurate data of performance. However, the present experiment will be useful to provide answers to the feasibility question of a plasma thruster of this type.

The thrust was measured by a pendulum-type thrust target.[7] A cone shape was chosen for the target, which would reduce any error caused by sputtered and rebounding particles. The target (cone diameter: 50 mm, length: 95 mm) was constructed of 0.2-mm-thick tungsten and was radiation cooled. A magnetic damper was attached to the bottom of the target and its deflection was determined optically with a cathetometer. In the present apparatus, the anode orifice diameter was sufficiently smaller than the cone diameter of the target, but the thruster diameter (anode holder diameter) was larger than it. So if the target is set too close to the thruster, the deflection of the target caused by rebounding particles between the thruster and the target becomes noticeable. If the target is set far from the thruster, it can not capture the spreading plasma beam completely. In order to